

This article was downloaded by:

On: 25 January 2011

Access details: *Access Details: Free Access*

Publisher *Taylor & Francis*

Informa Ltd Registered in England and Wales Registered Number: 1072954 Registered office: Mortimer House, 37-41 Mortimer Street, London W1T 3JH, UK



## Separation Science and Technology

Publication details, including instructions for authors and subscription information:

<http://www.informaworld.com/smpp/title~content=t713708471>

### Modeling of the Chromatographic Solvent Gradient Reversed Phase Purification of a Multicomponent Polypeptide Mixture

Lars Aumann<sup>a</sup>; Alessandro Buttè<sup>a</sup>; Massimo Morbidelli<sup>a</sup>; Klaus Büscher<sup>b</sup>; Berthold Schenkel<sup>b</sup>

<sup>a</sup> Department of Chemistry and Applied Biosciences, ETH Zurich, Institute for Chemical and Bioengineering, Zurich, Switzerland <sup>b</sup> NOVARTIS Pharma AG, Basel, Switzerland

**To cite this Article** Aumann, Lars , Buttè, Alessandro , Morbidelli, Massimo , Büscher, Klaus and Schenkel, Berthold(2008) 'Modeling of the Chromatographic Solvent Gradient Reversed Phase Purification of a Multicomponent Polypeptide Mixture', *Separation Science and Technology*, 43: 6, 1310 – 1337

**To link to this Article:** DOI: 10.1080/01496390801941026

URL: <http://dx.doi.org/10.1080/01496390801941026>

## PLEASE SCROLL DOWN FOR ARTICLE

Full terms and conditions of use: <http://www.informaworld.com/terms-and-conditions-of-access.pdf>

This article may be used for research, teaching and private study purposes. Any substantial or systematic reproduction, re-distribution, re-selling, loan or sub-licensing, systematic supply or distribution in any form to anyone is expressly forbidden.

The publisher does not give any warranty express or implied or make any representation that the contents will be complete or accurate or up to date. The accuracy of any instructions, formulae and drug doses should be independently verified with primary sources. The publisher shall not be liable for any loss, actions, claims, proceedings, demand or costs or damages whatsoever or howsoever caused arising directly or indirectly in connection with or arising out of the use of this material.

## Modeling of the Chromatographic Solvent Gradient Reversed Phase Purification of a Multicomponent Polypeptide Mixture

Lars Aumann,<sup>1</sup> Alessandro Buttè,<sup>1</sup> Massimo Morbidelli,<sup>1</sup>  
Klaus Büscher,<sup>2</sup> and Berthold Schenkel<sup>2</sup>

<sup>1</sup>Department of Chemistry and Applied Biosciences, ETH Zurich,  
Institute for Chemical and Bioengineering, Zurich, Switzerland

<sup>2</sup>NOVARTIS Pharma AG, Basel, Switzerland

**Abstract:** A model for Calcitonin purification from an industrial peptide mixture using polymer-based reversed phase columns was developed. Regressed competitive bi-Langmuir isotherm parameters for pure calcitonin are strong functions of the eluent composition and were correlated to the overall Henry coefficient only. It is shown that, by keeping constant these correlations, the adsorption behavior of impurities can be predicted simply by estimating their Henry coefficient from the raw mixture. The same can be repeated with very good results when changing the stationary phase or the organic solvent in the eluent. In both cases, only the Henry coefficient must be re-estimated from pulse injections.

**Keywords:** Reversed-phase chromatography, chromatographic modeling, peptide purification, multicomponent competitive adsorption isotherm, bi-Langmuir isotherm, solvent gradient chromatography

### INTRODUCTION

Solvent gradient chromatography is a powerful tool, widely used in industrial applications for the preparative purification of valuable bio-molecules, such as proteins and peptides. Since chromatographic purifications are typically cost

Received 17 July 2007, Accepted 23 December 2007

Address correspondence to Massimo Morbidelli, Department of Chemistry and Applied Biosciences, ETH Zurich, Institute for Chemical and Bioengineering, Zurich 8093, Switzerland. E-mail: morbidelli@chem.ethz.ch

intensive, significant improvements can be expected by applying model based optimizations. This is especially important for continuous preparative chromatographic purifications, such as the SMB process (1) or the Multicolumn Countercurrent Solvent Gradient Purification (MCSGP) process (2). For these reasons, the development of a reliable simulation model of the purification process is of paramount importance.

The accurate prediction of a chromatographic solvent gradient purification from a multicomponent mixture requires the knowledge of the adsorption equilibria as well as of the mass transport resistances inside the chromatographic column for all components involved. On the other hand, both the mixture and the pure product are often available only in small quantities and the isolation of all relevant impurities is generally very difficult and time consuming. Several techniques are available to estimate the relevant parameters required to run the model simulations. The adsorption isotherm can be evaluated by frontal analysis or batch experiments (3), by the perturbation method (4) or the inverse method (5). Among these, the inverse method is particularly attractive, because only small amounts of solute are required to perform the experiments at different mobile phase background compositions. The drawback of this method is that the type of the adsorption isotherm must be known *a priori*.

Many studies can be found in the literature, where the chromatographic separation of a mixture of well known solutes (typically up to three) is studied under isocratic or gradient elution conditions (6–11). In these cases, it is possible to proceed to the fitting of the relevant parameters after the isotherm expression and the set of mass balance equations have been defined. Moreover, methods which allow to estimate the retention behavior of the solutes based on their molecular structure are developing more and more (12–14). However, these approaches become extremely complex when working under typical industrial conditions. In this case, the feed mixture usually contains a large number of unidentified impurities. Additional problems come from the fact, that the feed composition can differ from batch to batch, and from the fact that preparative gradient elutions are typically performed close to column saturation conditions, where the competition among the different components is dominant. Therefore a robust, fast, and cheap methodology is desired, which must be able to estimate the isotherm parameters of the key-components in the multicomponent mixture with a reasonable experimental effort.

In this work a procedure is presented, which allows to predict solvent gradient purifications on a reversed phase system for a complex industrial polypeptide mixture. The procedure is based on the assumption that the components in the multicomponent mixture, however complex, have a “similar” adsorption behavior. According to this simplified assumption, once all isotherm parameters have been estimated in detail for the main component, the isotherms of all the impurities are simply related to the isotherm of the main component by means of their Henry constant value. This can be

estimated for the main impurities by means of simple isocratic retention time measurements under diluted conditions. This assumption appears to be especially realistic for those impurities, which elute closest to the product, i.e. the species which are eluted immediately before and after the main peak. These impurities will be in the following sections referred to as weakly and strongly adsorbing impurities, respectively, and they are the ones of largest interest for the process performance, being responsible for the final product purity. In addition to this, it is assumed that the mass transfer resistance of all impurities is identical to the one of the main component. The consequences of these assumptions are:

- i. a strong reduction of the experimental effort for evaluating the model parameters,
- ii. a similar reduction in the number of input parameters and
- iii. the need of using only small amounts of the raw materials and of not isolating the single impurities.

Accordingly, the aim of this work is to discuss to which extent the previous strategy is able to produce reliable prediction of the elution behavior of a complex industrial mixture. To further validate this strategy, additional tests will be performed by using a single model impurity (Insulin), by changing the stationary phase and by changing the organic modifier in the mobile phase.

## CHROMATOGRAPHIC MODEL

A classical lumped pore diffusion model will be used in this work. This is possible, since the characteristic time of diffusion is much faster than the characteristic time of convection. According to this model, the main mass transfer resistances are represented by an external film diffusion transfer and a lumped linear diffusion resistance inside the particle liquid pores.

The following set of mass balance equations are written for each component in the system:

$$\frac{\partial c_i}{\partial t} + \frac{(1 - \varepsilon_b)}{\varepsilon_b} k_L (c_i - c_{p,i}) + \frac{u_{sf}}{\varepsilon_b} \frac{\partial c_i}{\partial z} = D_{ax} \frac{\partial^2 c_i}{\partial z^2} \quad (1)$$

$$\varepsilon_p \frac{\partial c_{p,i}}{\partial t} + (1 - \varepsilon_p) \frac{\partial q_i}{\partial t} = k_L (c_i - c_{p,i}) \quad (2)$$

where  $c_i$  is the concentration in the mobile phase of the  $i$ -th solute,  $c_{p,i}$  its concentration in the stagnant phase inside the particles,  $q_i$  the equilibrium concentration in the solid.  $\varepsilon_b$  is the bed porosity, whereas  $\varepsilon_p$  the accessible pore fraction in the particles. The latter can change with the molecular size of each component. However, for the sake of simplicity, it is kept constant for

each component in this work. The same can be said for the transport coefficients:  $k_L$ , the lumped mass transfer coefficient between the mobile and the stagnant phase and  $D_{ax}$ , the axial effective diffusion. Both are kept constant for all the components.

Previous mass balance equations must be coupled with the following initial and boundary conditions for the mobile phase:

$$\begin{aligned} c_i(t=0, z) &= 0 & \text{for } 0 < z < 1 \\ \frac{\partial c_i(t, z=0)}{\partial t} &= \frac{u_{sf}}{D_{ax}}(c_{f,i}(t) - c_i(t, z=0)) & \text{for } t > 0 \\ \frac{\partial c_i(t, z=L)}{\partial t} &= 0 & \text{for } t > 0 \end{aligned} \quad (3)$$

and for the stagnant phase:

$$c_{p,i}(t=0, z) = 0 \quad \text{for } 0 < z < 1 \quad (4)$$

where  $c_{f,i}$  is the feed concentration (for  $z \rightarrow -\infty$ ) of the  $i$ -th component.

The inorganic modifier or acid ( $H_3PO_4$ ) is supposed not to adsorb on the stationary phase, i.e.  $q = 0$  always. The organic modifiers (acetonitrile or methanol) are supposed to follow a non-competitive Langmuir adsorption isotherm. In other words, their adsorption behavior is not influenced by the presence of the other solutes. This is not true for the solutes, whose equilibrium adsorption concentrations,  $q_i$ , is computed using the following competitive bi-Langmuir isotherm:

$$q_i = \frac{H_{1,i}c_{p,i}}{1 + \sum_{j=1}^N (H_{1,j}/q_{1,j}^\infty)c_{p,j}} + \frac{H_{2,i}c_{p,i}}{1 + \sum_{j=1}^N (H_{2,j}/q_{2,j}^\infty)c_{p,j}} \quad (5)$$

where  $H_{l,i}$ , the Henry coefficient for the  $l$ -th site ( $l = 1, 2$ ) of the  $i$ -th component, and  $q_{l,j}^\infty$ , the corresponding saturation capacity, are both functions of the eluent composition, i.e. of the local concentration of organic and inorganic modifier.  $N$  is the number of solutes in the mixture.

Most of the transport parameters have been estimated by available literature correlations. In particular, the axial dispersion is estimated using the following expression (3):

$$D_{ax} = \gamma_1 D_m + \gamma_2 d_p \frac{u_{sf}}{\varepsilon_b} \quad (6)$$

where  $\gamma_1 = 0.7$  and  $\gamma_2 = 0.5$  are two constants,  $d_p$  the particle (bead) diameter and  $D_m$  the molecular diffusivity. The lumped liquid mass transfer coefficient  $k_L$  consists of two mass transfer resistances in series: the effective external film,  $\bar{k}_f$ , and lumped pore mass transfer coefficient,  $\bar{k}_p$ :

$$\frac{1}{k_L} = \frac{1}{\bar{k}_f} + \frac{1}{\bar{k}_p} \quad (7)$$

where  $k_f$  and  $k_p$  have been defined as (3)

$$\bar{k}_f = \frac{6}{d_p} k_f \quad (8)$$

$$\bar{k}_p = \frac{60}{d_p^2} D_{\text{eff}} \quad (9)$$

The external film transfer coefficient  $k_f$  in Eq. (8) is estimated using the equation of Wilson and Geankolis (3):

$$Sh = \frac{1.09}{\varepsilon} [\text{Re } Sc]^{1/3} \quad (10)$$

The value of the effective pore diffusivity,  $D_{\text{eff}}$  Eq. (9) is the only regressed mass transport parameter. Its value has been estimated by regression of diluted isocratic pulse injections of calcitonin at different velocities (experiment not reported) and has been set to  $3.3 \cdot 10^{-7} \text{ cm}^2/\text{s}$ .

## EXPERIMENTAL PART

### The Purification Problem

Calcitonin is a peptide hormone produced by the parafollicular cells of the thyroid gland in mammals and by the ultimobranchial gland of birds and fishes (15, 16). Salmon Calcitonin, which is more potent and longer lasting than the human one, has been widely used for the treatment of osteoporosis, paget's disease, hypercalcemic shock and chronic pain in terminal cancer patients. It has a molecular weight of 3432 g/mol.

Salmon Calcitonin has been supplied by NOVARTIS Pharma AG Basel, Switzerland. The raw Calcitonin has been taken out of the production process, so that a real industrial multicomponent mixture could be investigated. An analytical chromatogram of the original peptide mixture is shown in Fig. 1. The mixture consists of ca. 30% weakly adsorbing impurities, 46% Calcitonin and ca. 24% of strongly adsorbing impurities. The analytical chromatogram has been recorded on the analytical column ZORBAX 300-SB,  $150 \times 4.6 \text{ mm}$  with  $5 \mu\text{m}$  particle diameter at  $60^\circ\text{C}$ .

In order to reduce the complexity of the purification problem, key-components have been defined, which consist of several impurities showing similar adsorption behavior on the preparative resin, and therefore eluting more closely to the Calcitonin peak. Fractions of key components, which are not necessarily constituted by single components, are collected during a preparative elution and they have been reinjected at different mobile phase compositions to evaluate the Henry constant of the impurity group. The definition of these key-components is shown in Fig. 1 and indicated as  $W_1$  to  $W_3$  for the weak impurities and  $S_1$  and  $S_2$  for the strong ones.

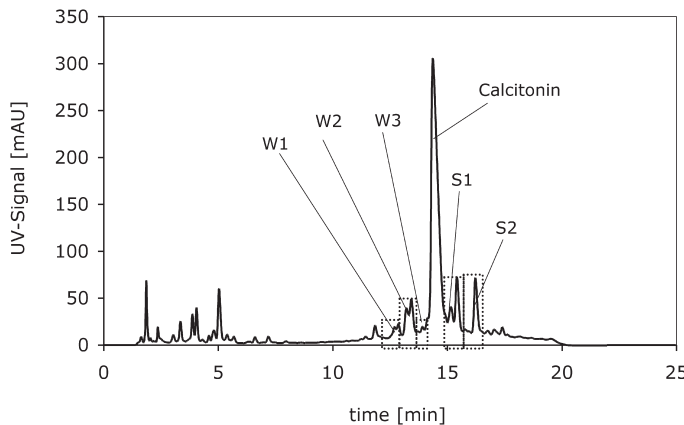


**Figure 1.** Analytical chromatogram of raw Calcitonin. Weakly and strongly adsorbing impurities need to be separated from the intermediate fraction. Groups of impurities, which show similar retention behavior have been defined as weakly adsorbing  $W_1$  to  $W_3$  and strongly adsorbing  $S_1$  and  $S_2$  key-impurities, respectively.

Calcitonin has been also provided as a powder, whose purity is about 90%. This calcitonin has been used to carry out over-loaded experiments. On the other hand, the Calcitonin used to carry out diluted experiments has been purified on a preparative column starting from the original mixture. Its purity is about 97%.

### Preparative Stationary Phases

The stationary phase for the preparative purification is “Source 15RPC” by GE Healthcare, a mono-disperse highly porous material with an average pore diameter of ca. 2000 Å and a particle size of 15 µm. Note that, since a large range of modifier concentration and consequently of Henry constant values will be explored, columns with different length are needed, as detailed in Table 1. In addition, isotherm and mass transfer parameters have been measured also for the resin “PLRP-S” by Polymer Laboratories, which has the identical chemical composition (cross-linked polystyrene/DVB copolymer) but an internal average pores size of ca. 300 Å and a particle size of 10 µm (cf Table 1).

In Table 1, the porosities of the analyzed columns are reported. The bed porosity has been measured by pulse injections of a polyethylene glycol standard with an average molecular weight of 100000 g/mol and using 300 g/L acetonitrile and 2 mg/g of H<sub>3</sub>PO<sub>4</sub> in the eluent. The total porosity has been measured under the same conditions using water, sodium nitrate or thiourea. Finally, the total accessible porosity of Calcitonin has been

**Table 1.** Dimensions and porosities of the preparative columns used in this work.  $\varepsilon_{\text{calc}}$  refers to the total accessible porosity of Calcitonin

Column No.	Resin	Dimension	$d_p$	$\varepsilon_b$	$\varepsilon_{\text{calc}}$	$\varepsilon_{\text{total}}$
1	PLRP-S 300 <sup>a,c</sup>	250 × 4.6 mm	10 $\mu\text{m}$	0.32	0.54	0.63
2	Source 15 RPC <sup>b,c</sup>	100 × 6.4 mm	15 $\mu\text{m}$	0.40	0.66	0.78
3	Source 15 RPC <sup>b,d</sup>	20 × 3 mm	15 $\mu\text{m}$	0.40	0.66	0.78
4	Source 15 RPC <sup>b,d</sup>	100 × 4.6 mm	15 $\mu\text{m}$	0.40	0.66	0.78

<sup>a</sup>Supplied by polymer laboratories;

<sup>b</sup>Supplied by GE healthcare;

<sup>c</sup>Commercial (pre-packed) column;

<sup>d</sup>Self-packed column.

measured using 400 g/L of acetonitrile in the mobile phase, since at 300 g/L a little adsorption can be measured. The measured value for the Source 15 RPC stationary phase ( $\varepsilon = 0.66$ ) is indicating that about 68% of the total particle porosity is actually accessible to calcitonin. This values raises to about 71% in the case of PLRP-S 300.

## Experimental Equipment

The experiments are carried out on an Agilent HP1100 HPLC system, equipped with a gradient pump module, a degasser, an autosampler, a column temperature control and a diode-array detector to monitor simultaneously several wavelengths. The mobile phase used for the purification consists of water, acetonitrile, and phosphoric acid ( $\text{H}_3\text{PO}_4$ , MERCK, UN 1805). De-ionized water was purified with a “Synergy” water purification system by MILLIPORE. No buffer is used. The different mobile phase compositions are obtained by mixing two different solvents: Solvent A, 100.5 g of acetonitrile, 868.1 g of water; Solvent B, 455.6 g of acetonitrile, 414.5 g of water. Both solvents contain 2 mg/g of  $\text{H}_3\text{PO}_4$ .

## Adsorption Isotherm of the Modifier

The perturbation method has been used to determine the adsorption isotherm of the organic modifier (4). Small volumes of acetonitrile have been injected into the column at different background compositions of acetonitrile and the perturbation is monitored at a wave length of 192 nm. The isotherm for the concentration interval of interest can be approximated with a Langmuir isotherm:  $H = 1.6$  and  $q_{\text{sat}} = 260 \text{ g/l}$ .

## RESULTS AND DISCUSSION

## Adsorption Isotherm of Pure Calcitonin

In the following, the adsorption isotherm of pure calcitonin is determined as a function of the mobile phase composition. Different experiments are carried out under diluted or overloaded pulse injections, using isocratic or linear gradient elution conditions, in order to regress the parameters of Eq. (5).

## Diluted Isocratic Elutions

The overall Henry constant ( $H_{\text{Calc}} = H_1 + H_2$ , cf Eq. (5)) of Calcitonin adsorption isotherm has been evaluated from the average elution time of pure Calcitonin for several background compositions of modifier using isocratic elution conditions and very diluted pulse injections, so to operate in the linear region of the bi-Langmuir isotherm (3). The results obtained on column 3 (squares) and 4 (diamonds) are shown as function of the modifier concentration in Fig. 2. To further account for the influence of phosphoric acid, the Henry constant has additionally been evaluated at a constant acetonitrile content of 222 g/l as function of the acid mass fraction in the mobile phase. The comparison between experimental and correlated Henry values is shown in Fig. 3.

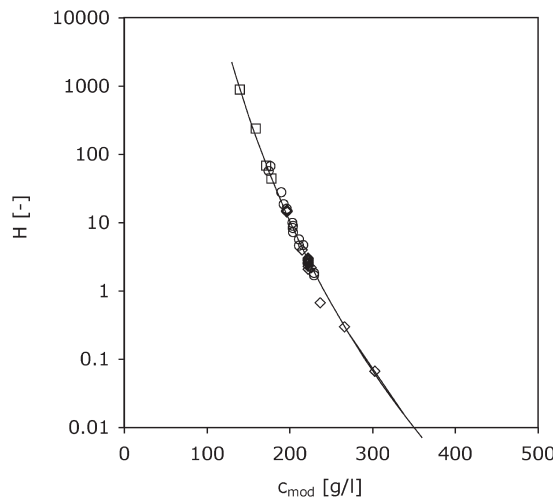


**Figure 2.** Henry constant of Calcitonin as function of the modifier concentration in the mobile phase. Constant phosphoric acid mass fraction of  $x_{\text{H}_3\text{PO}_4} = 2 \text{ g/kg}$ . Circles: overloaded isocratic peak fitting on “Column 1” and “Column 2”; squares: diluted isocratic elutions on “Column 3”; diamonds: diluted isocratic elutions on “Column 4”, solid curve: correlation for both resins according to Eq. (11).

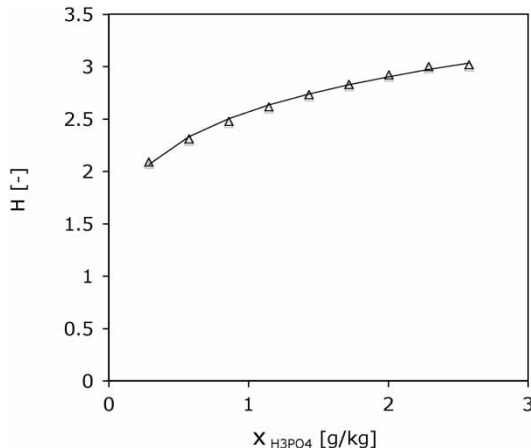


**Figure 3.** Experimental Henry constant of Calcitonin as a function of the phosphoric acid content in the mobile phase measured on “Column 1” under diluted conditions for an acetonitrile concentration of 222 g/l in the mobile phase. The curve represents the results of the correlation Eq. (11).

The dependency of the Henry constant of calcitonin on the mobile phase composition can be described by means of a simple power function, under the assumption that the effects of the organic and inorganic modifier are independent of each other:

$$H_i = A_{H,i} (x_{H_3PO_4})^{D_{H,i}} (c_{mod})^{B_{H,i}} \quad (11)$$

where  $c_{mod}$  indicates the organic modifier (acetonitrile). The values of the regressed parameters are reported in Table 2.

**Table 2.** Regressed parameter values using acetonitrile as organic modifier

Parameter	Regressed values		
$H_{\text{Calc}}$ Eq. (11)	$A_{H,\text{Calc}} = 1.27 \cdot 10^{30}$	$B_{H,\text{Calc}} = -12.43$	$D_{H,\text{Calc}} = 0.175$
$H_{\text{Calc}}$ Eq. (11) <sup>a</sup>	$A_{H,\text{Calc}} = 2.19 \cdot 10^{34}$	$B_{H,\text{Calc}} = -13.47$	$D_{H,\text{Calc}} = 0$
$H_{\text{Ins}}$ Eq. (11)	$A_{H,\text{Ins}} = 1.315 \cdot 10^{45}$	$B_{H,\text{Ins}} = -19.19$	$D_{H,\text{Ins}} = 0$
$H_2$ Eq. (12)	$A_{H_2} = 0.232$	$B_{H_2} = 0.794$	
$q_1^\infty$ Eq. (14)	$A_{q_1^\infty} = 37.78$	$B_{q_1^\infty} = 0.2$	$D_{q_1^\infty} = 0.6521$
$q_2^\infty$ Eq. (14)	$A_{q_2^\infty} = 11.37$	$B_{q_2^\infty} = 0.3$	$D_{q_2^\infty} = 0.1926$

<sup>a</sup>Ethanol used as organic modifier.

### Overloaded Isocratic Elutions

To explore the non-linear region of the adsorption isotherm of Calcitonin, overloaded isocratic elution profiles have been recorded at several mobile phase compositions. All regressed isotherm parameters show a strong dependence on the mobile phase composition. Instead of correlating the isotherm parameters to the mobile phase composition, the Henry constant of the second adsorption site  $H_2$  has been correlated to the overall Henry constant of calcitonin  $H_{\text{Calc}}$  (cf. Eq. (11)), while the local saturation capacities  $q_1^\infty$  and  $q_2^\infty$  have been correlated to the corresponding local Henry constants,  $H_1$  and  $H_2$ , respectively:

$$H_2 = A_{H_2}(H)^{B_{H_2}} \quad (12)$$

$$q_i^\infty = A_{q_i^\infty}(H_i)^{B_{q_i^\infty}} \quad (13)$$

It is worth noting that the subscript Calc referring to Calcitonin is no more present in previous expressions. In fact, these equations are general for the system investigated and will be used for all the components, as discussed later.

Nine isocratic overloaded elution profiles have been recorded on "Column 1", changing the acetonitrile concentration between 174.5 and 229.3 g/l, and seven profiles on "Column 2", between 193 and 207 g/l. All isocratic overloaded elutions have been carried out at a constant phosphoric acid mass fraction ( $x_{\text{H}_3\text{PO}_4} = 2 \text{ mg/g}$ ). For each condition, four parameters have been regressed,  $H_i$  and  $q_i^\infty$  ( $i = 1, 2$ ), in spite of the fact that the overall Henry coefficient has been already regressed in the diluted isocratic experiments. In Figure 4 the regressed local Henry constants for the first and the second adsorption sites are shown as a function of the mobile phase composition.  $H_2$  shows a strong scatter for values below one, which could be due to the fact, that under the conditions investigated the adsorption on the second site is still close to the linear adsorption region. For this reason, it was not possible to regress the value of  $q_2^\infty$ , which will be estimated later using overloaded linear gradient elution elutions. To double-check the quality of the regression, the overall Henry constant has been estimated from the regressed  $H_i$  values and compared (circles) with the values obtained under diluted conditions in Fig. 2. It can be observed that the agreement between the two sets of data is excellent.

The regressed saturation capacity of the first site using different acetonitrile concentrations (i.e., different values of the total Henry coefficient, according to Eq. (11) are shown in Fig. 5, where the correlation equation (13) is also shown (solid curve). The values of the saturation capacity  $q_1^\infty$  appear to be small and relatively small scattered. However, the extrapolation using the correlation Eq. (11) to larger values of  $H_{1,\text{Calc}}$  might contain large error. On the other hand, as it will be discussed in the following section, in

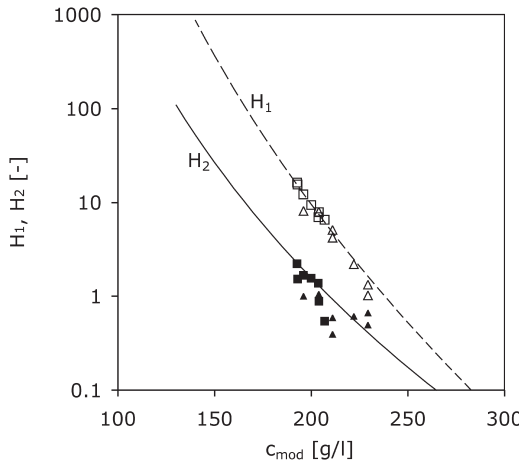


**Figure 4.** Regressed Henry constants for both adsorption sites on “Column 1” and “Column 2”. Solid line: correlation for  $H_2$ ; dashed line: correlation for  $H_1$ ; empty squares:  $H_1$  on “Column 2”; empty triangles:  $H_1$  on “Column 1”; filled squares:  $H_2$  on “Column 2”; filled triangles:  $H_2$  on “Column 1”.

this range of acetonitrile concentration, most of the capacity is in the second adsorption site. In order to estimate  $q_2^\infty$ , much larger injection volumes of Calcitonin are needed, which become soon impractical under isocratic conditions. For this reason, linear gradient elutions will be used.

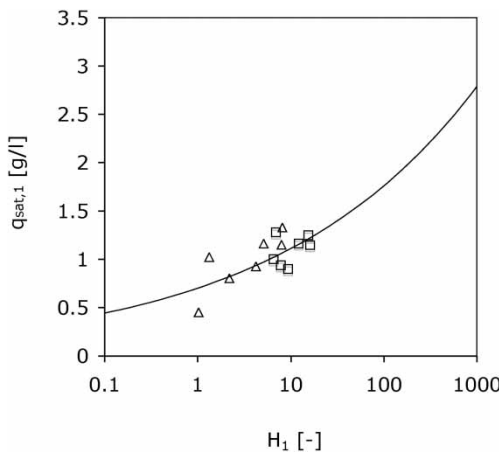


**Figure 5.** Regressed saturation capacity of the first adsorption site for Calcitonin as a function of the corresponding Henry constant  $H_1$ . Solid curve: correlation; squares: “Column 2”; triangles: “Column 1”.

### Overloaded Linear Gradient Elutions

A single solvent linear gradient elution has been carried out with pure Calcitonin on “Column 1” with the aim of regressing the saturation capacity of the second adsorption site,  $q_2^\infty$ . All the remaining parameters, which have been already regressed from isocratic elutions, are kept constant. Following the same strategy as for the saturation capacity of the first site,  $q_2^\infty$  is regressed according to Eq. (13). The comparison between the experimental linear gradient elution profile and the best model simulation is shown in Fig. 6. It can be noted, that the agreement with the model is very satisfactory. The need for using a bi-Langmuir isotherm can be clearly seen in Fig. 6, where the tail of the overloaded peak presents a clear discontinuity between two linear trends at about 23 min elution time.

### Influence of the Phosphoric Acid Content on the Saturation Capacities

Before proceeding with the model validation, it must be again mentioned that the retention behavior of Calcitonin is largely influenced by the phosphoric acid content in the mobile phase. In order to account for this dependence, the saturation capacity of the two sites, Eq. (13), has been redefined as in the following, in a similar fashion to what was done for the total Henry

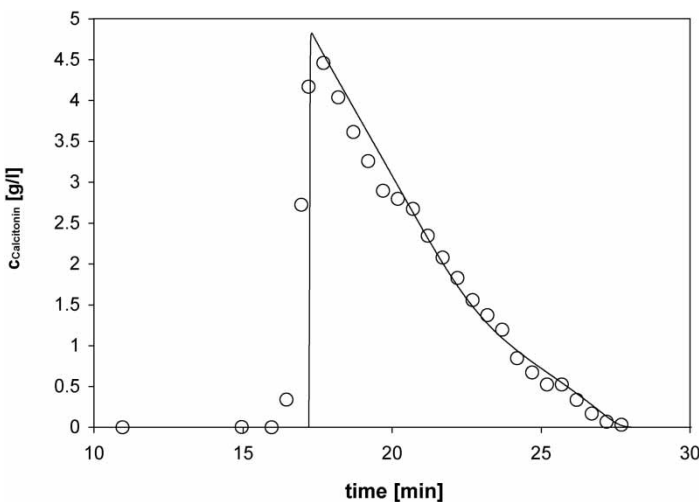


**Figure 6.** Experiment and simulation of the overloaded solvent gradient elution of pure Calcitonin on “Column 1”. Linear solvent gradient from 138 to 357.3 g/l acetonitrile from 5 to 35 minutes. Injection of  $4 \times 99 \mu\text{l}$  of 24.6 g/l pure Calcitonin.  $x_{\text{H}_3\text{PO}_4} = 20 \text{ g/kg}$ .  $Q = 0.5 \text{ ml/min}$ . Circles: experimental analyses with HPLC; solid curve: simulated peptide concentration at the column outlet.

coefficient (cf Eq. (11)):

$$q_i^\infty = A_{q_i^\infty} (x_{H_3PO_4})^{D_{q_i^\infty}} (H_i)^{B_{q_i^\infty}} \quad (14)$$

An experiment has been carried out, where the acetonitrile concentration was kept constant at 197 g/l, while the phosphoric acid content has been linearly changed from 4.0 to 0.22 mg/g  $H_3PO_4$  in 10 minutes. It should be noted that, in contrast to the modifier, whose adsorption behavior is described by a Langmuir isotherm, the acid is assumed not to adsorb. A comparison between simulation (solid thick curve) and experiment (circles) is shown in Fig. 7 for three different injection volumes of calcitonin. The model prediction matches well with the experiment and this demonstrates the suitability of the model. The negative peak in the simulated phosphoric acid concentration profile (solid thin curve) at around 3 minutes is due to a different acid content between the sample vial (1.0 mg/g  $H_3PO_4$ ) and the eluent (4.0 mg/g). In order to appreciate the effect of the acid content on the adsorption isotherm, in Table 3 the changes in Henry coefficient and saturation capacity at the beginning and at the end of the acid gradient are reported, respectively.

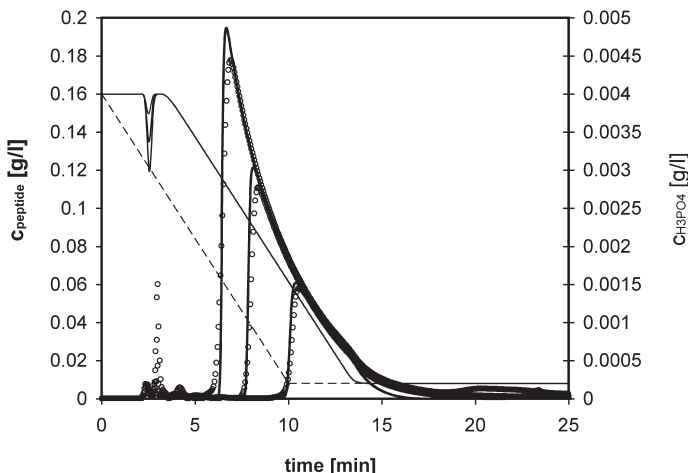


**Figure 7.** Comparison between simulations and experimental chromatograms for a phosphoric acid gradient in “Column 2”. Injection of 30, 60 and 99  $\mu$ l of 6.3 g/l Calcitonin at 197 g/l acetonitrile. Acid gradient from 0.004 – 0.0002 g/kg in 10 minutes.  $Q = 1.0$  ml/min. Thick curves: simulated calcitonin profiles; dashed curve: outlet modifier concentration; thin curve: simulated modifier profile at column outlet; circles: calibrated UV-signals at 220 nm.

**Table 3.** Influence of the phosphoric acid concentration in the mobile phase on the isotherm parameters of pure Calcitonin for a constant modifier content of 197 g/l

	$x_{\text{H}_3\text{PO}_4}$	$H_1$	$q_{\text{sat},1}$	$H_2$	$q_{\text{sat},2}$
Gradient start	0.004	12.4	1.8 g/l	1.9	8.7 g/l
Gradient end	0.0002	7.2	0.2 g/l	1.3	4.2 g/l

### Model Validation with Pure Calcitonin

Four gradient elutions on “Column 2” have been carried out using different gradient slopes and three different injection volumes of Calcitonin. A comparison between simulated prediction and calibrated UV-Signal at “280 nm” is shown in Fig. 8. The agreement between predictions and experiments is excellent. The hump close to the elution tails of the elution profiles is due to the impurities  $S_1$  and  $S_2$ , which have not been accounted for in these simulations. This set of experiments confirms the quality of the regressions on the adsorption isotherm for Calcitonin performed in the previous sections.

An additional linear gradient elution run has been carried out at a different content of acid in the two solvents (4.0 g/kg  $\text{H}_3\text{PO}_4$ ). Also, in this case the agreement between experiments and model prediction is very satisfactory, as it can be appreciated in Fig. 9.

Thus summarizing, all isotherm parameters of pure Calcitonin have been evaluated as a function of the modifier and the phosphoric acid content in the mobile phase. The different isotherm parameters have been then correlated to the total Henry coefficient of Calcitonin. This simplified model, which is lumping several effects as the change in porosity as a function of the acetonitrile concentration, is able to well predict the elution of pure calcitonin under different operative conditions. This result has been obtained with a very limited number of experiments and, in particular, using a very limited amount of pure calcitonin.

### Introduction of Main Impurities of the Raw Mixture

#### Henry Constants of the Key-Impurities

Retention times for the key-impurities identified in Fig. 1 have been measured by diluted isocratic experiments at different mobile phase compositions in order to evaluate the Henry constants for each impurity and, thus, the corresponding selectivity with respect to Calcitonin,  $S_i = H_i/H_{\text{Calc}}$ . This has been done both by injecting the raw mixture under very diluted conditions and, as a comparison, by injecting separately the different impurities isolated from overloaded gradient experiments. The obtained results do not

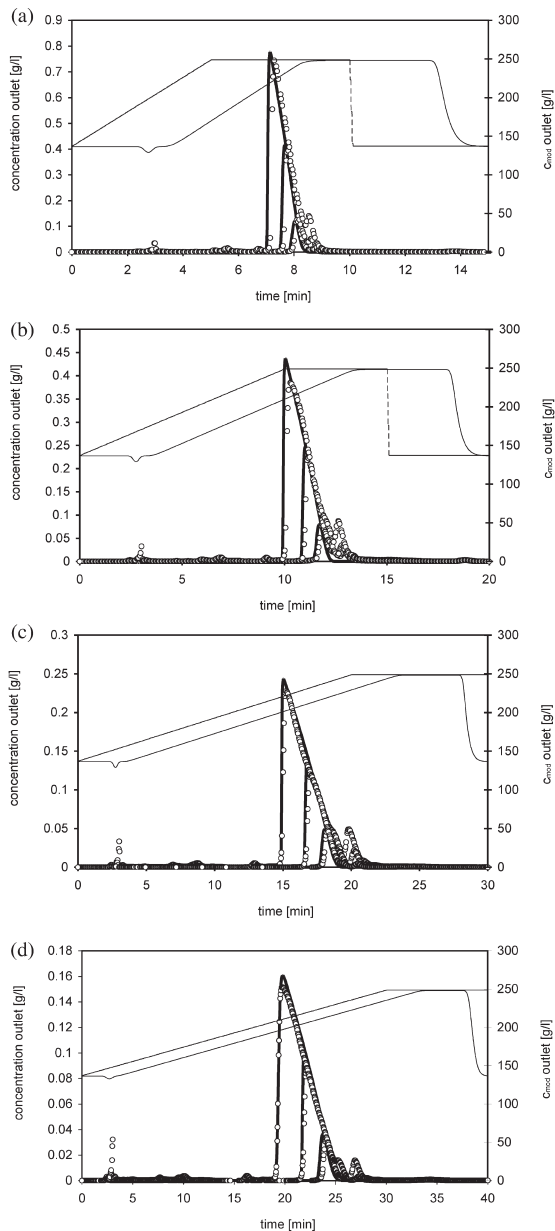


**Figure 8.** Gradient elution experiments of pure calcitonin from 137 to 248 g/l acetonitrile in (a) 5, (b) 10, (c) 20 and (d) 30 minutes. Injection of 5, 25 and 75  $\mu$ l of 7 g/l 90% pure Calcitonin.  $x_{\text{H}_3\text{PO}_4} = 4.0 \text{ g/kg}$ ,  $Q = 1.0 \text{ ml/min}$ . The dashed line represents the solvent gradient at the pump outlet and the thin line shows the simulated modifier outlet concentration for the largest injection volume. The dots represent the calibrated UV-signal at 280 nm wavelength and the thick curves are the model predictions.

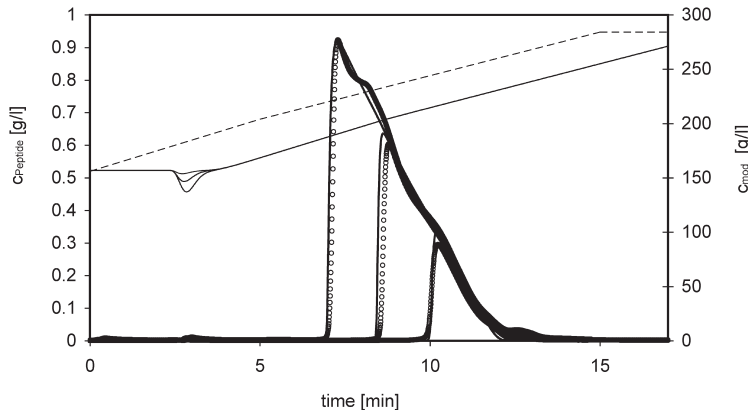


**Figure 9.** Gradient elution experiments of pure calcitonin of pure Calcitonin on “Column 2”. Linear solvent gradient: 157 to 204.33 g/l acetonitrile from 0 to 5 minutes, 204.33 to 284.7 g/l acetonitrile from 5 to 15 minutes. Injection of 60, 99, and  $2 \times 99 \mu\text{l}$  of 11.8 g/l pure Calcitonin.  $x_{\text{H}_3\text{PO}_4} = 4.0 \text{ g/kg}$ ,  $Q = 1.0 \text{ ml/min}$ . Circles: calibrated UV-signal at 280 nm; thick solid curve: simulated peptide concentration at column outlet; dashed curve: modifier concentration at pump inlet, thin solid curve: simulated modifier profile at column outlet. The sample vial contains ca. 110 g/l acetonitrile.

vary significantly, indicating that due to their low concentration the impurities are always in the linear range of their adsorption isotherm. The selectivity of the impurities is shown as function of the Henry constant of Calcitonin in Fig. 10. There is little data scattering, mainly due to the fact that key impurities are often partially overlapping and are not necessarily made of pure components. In spite of this, a clear dependence of selectivity on the modifier content can be observed, especially for the strongly adsorbing impurities. A similar clear dependence to the phosphoric acid content could not be found. Only for the impurity  $S_1$  a slight increase in the selectivity has been observed for decreasing the phosphoric acid contents.

The selectivities have been regressed as function of the Henry constant of Calcitonin using the following power function:

$$S_i = \frac{H_i}{H_{\text{Calc}}} = A_{S,i} (H_{\text{Calc}})^{B_{S,i}} \quad (15)$$

where  $H_i$  is the total Henry coefficient of the  $i$ -th impurity. The regressed coefficient values are reported in Table 4. Note, that also in this case no difference is observed for the two considered stationary phases indicated as “Column 1” and “Column 2” according to Table 1.

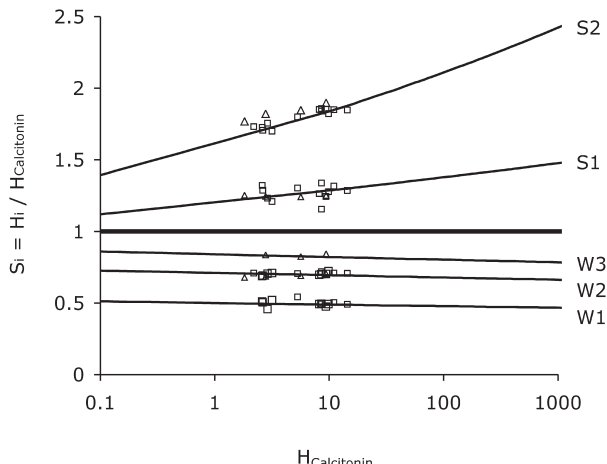


**Figure 10.** Selectivities of impurities with respect to Calcitonin. Curves: Equation (15); squares: experimental selectivity measured on “Column 2”; triangles: experimental selectivity measured on “Column 1”.

### Purification of the Raw Peptide Mixture

As mentioned in the Introduction, in this work it is suggested that effective predictions of the elution of a peptide mixture can be obtained by measuring the overall Henry coefficient only for each single impurity, while applying all the remaining correlations developed for pure calcitonin. More specifically, Eqs. (12), (14) and the additional equation  $H_i = H_{1,i} + H_{2,i}$  will be applied with the coefficients summarized in Table 2. Moreover, the same mass transport coefficient for all the components are used.

In Figure 11 the experimental elution profile for an overloaded gradient elution experiment with raw Calcitonin is shown. The elution profiles of the weakly (W1 to W3) and of the strongly adsorbing impurities (S1 and S2) are shown, together with the peak corresponding to Calcitonin. Experiments are compared to the simulated elution curves for the same components. The

**Table 4.** Coefficients to compute the selectivity of impurities with respect to Calcitonin using Eq. (15)

Name	$A_{S,i}$	$B_{S,i}$
W1	0.50	-0.01
W2	0.71	-0.01
W3	0.84	-0.01
S1	1.20	0.03
S2	1.6	0.06

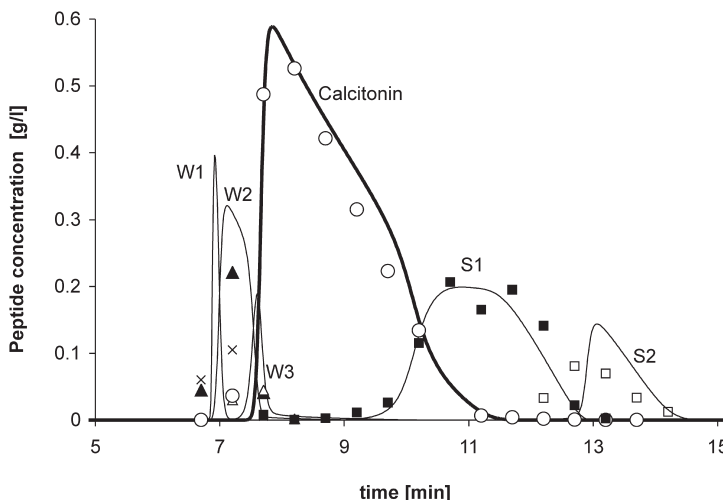


**Figure 11.** Simulated and experimental chromatograms for Calcitonin and for weakly (W1, W2, W3) and strongly (S1 and S2) impurities for a solvent gradient elution on “Column 2”. Injection of 40  $\mu$ l of 65 g/l raw Calcitonin. Gradient from 180 to 284 g/l acetonitrile in 15 minutes.  $Q = 1.0$  ml/min. Thin solid curves: simulation profiles of key impurities; thick solid curves: simulation profile of Calcitonin; crosses: impurity W1 (2% of feed); filled triangles: impurity W2 (7% of feed); empty triangles: impurity W3 (2% of feed); circles: Calcitonin (46% of feed); filled squares: impurity S1 (17% of feed); empty squares: impurity S2 (5% of feed).

general agreement between the model and the experiments is satisfactory, especially when considering that the extrapolation of the selectivities for each impurity to large adsorption conditions may be imprecise (cf Fig. 10). In particular, a good agreement is found for Calcitonin. In front of the Calcitonin peak, the simulation predicts a very sharp displacement effect of the weakly adsorbing impurities. This behavior seems confirmed by the experiments, although the difficulties connected to the isolation and the quantification of the single impurities make this comparison difficult to be evaluated. The behavior in the Calcitonin peak tail is clearer. Here, both the experiments and the simulation show a weak displacement of the key-impurity S<sub>1</sub>. As for the weakly adsorbing impurities, the comparison on S<sub>2</sub> is difficult to judge, even if the position of this peak appears to be well predicted.

#### Binary Separation of Calcitonin and Insulin

In this section, a deeper insight into the proposed approach of using all the correlation developed for pure calcitonin for other impurities, with the only exception of the overall Henry coefficient, is given. To this regard, it has

been decided to investigate the purification of Calcitonin and Insulin, where Insulin was taken as a convenient model impurity, due to the fact that it is available in pure state.

### Adsorption Characterization of Pure Insulin

Insulin (*SIGMA-ALDRICH, no. I-2643*) has a molecular mass of 5808 g/mol, that is 1.7 times heavier than Calcitonin. Significant differences in the adsorption isotherm parameters with respect to Calcitonin are expected.

The total accessible porosity for Insulin on "Column 2" is equal to  $\varepsilon = 0.65$ . This is only slightly smaller than that for Calcitonin, so that size exclusion effects are negligible. The Henry coefficient for Insulin has been measured under diluted isocratic conditions and, additionally, via peak fitting of overloaded isocratic elutions at different mobile phase compositions, that is using the same procedure as for Calcitonin. All experiments have been carried out at  $x_{\text{H}_3\text{PO}_4} = 2.0 \text{ g/kg}$ . The Henry constant of Insulin is shown in Fig. 12 (filled circles) and compared with the one measured for Calcitonin (open squares) on the same column and the same conditions. It can be seen that the total value of the Henry constant in the region of interest is similar for both molecules, but the slope with respect to the modifier concentration is larger for Insulin. A selectivity reversal between Calcitonin and Insulin occurs at about 190 g/l acetonitrile, where the two curves cross each other. The overall Henry constant of Insulin was regressed using the same expression

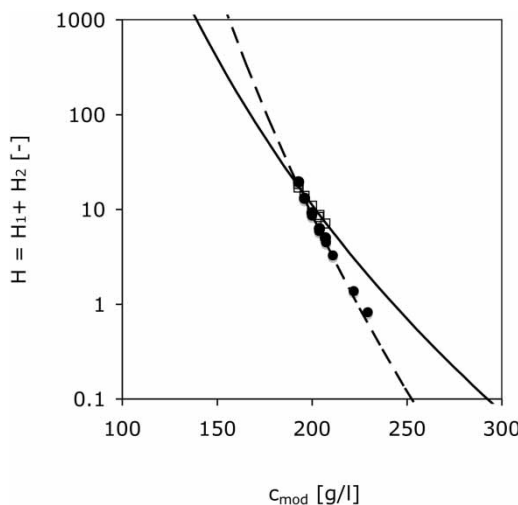


**Figure 12.** Overall Henry constant for Calcitonin and Insulin as a function of the acetonitrile concentration evaluated on "Column 2" for  $x_{\text{H}_3\text{PO}_4} = 2.0 \text{ g/kg}$ ; squares: Calcitonin; filled circles: Insulin, thickline: correlation for Calcitonin Eq. (11); dashed line: correlation for Insulin Eq. (11).

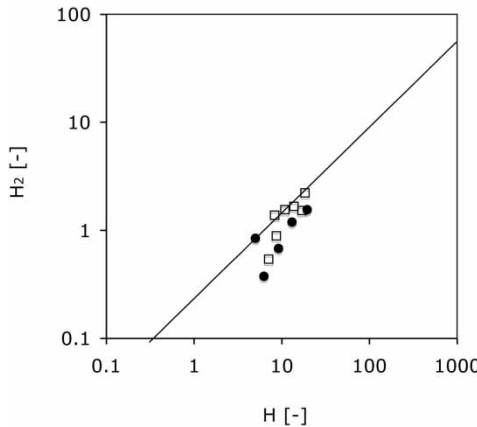


**Figure 13.** Henry constant for the second adsorption site of Calcitonin and Insulin as a function of the corresponding overall Henry constant evaluated on “Column 2” for  $x_{H_3PO_4} = 2.0$  g/kg. Filled circles: Insulin; squares: Calcitonin; line: Eq. (12).

as for Calcitonin (cf Eq. (11)), although the dependence upon the acid content is ignored (i.e.,  $D_{H, Ins} = 0$ ). The regressed parameter values are reported in Table 2.

Five overloaded isocratic elution profiles have been carried out in order to regress the remaining bi-Langmuir isotherm parameters. The values of  $H_2$  (filled circles) regressed from these experiments are shown in Fig. 13 as a function of the corresponding overall Henry constant,  $H_{Ins}$ . In the same graph, the dependency of  $H_2$  on  $H_{Calc}$  is shown (open squares). It can be observed, that in spite of the very different behavior of the overall Henry values of the two components, a similar correlation is found. The same is valid for the saturation capacity of the first adsorption site, where no strong deviation from the correlation measured for Calcitonin can be observed, as shown in Fig. 14.

Thus summarizing, although Calcitonin and Insulin have a very different chemical structure and behavior, their adsorption isotherm parameters show very similar behavior, when represented as a function of the corresponding overall Henry constant. To further proof this concept, a solvent gradient elution of Insulin was carried out and compared to the model prediction for two different injection volumes in Fig. 15. The same solvent gradient used in Fig. 8(d) has been used in this case. The agreement between the experiments and model predictions is very good, especially when considering that this result was obtained by using only two regressed parameters: the overall Henry constant and the accessible porosity. All the remaining correlations are those developed for Calcitonin, including the mass transport parameters. This result is even more significant, if the elution profiles of Insulin are compared to those found for Calcitonin under the same conditions, which are represented by the thin lines in the same figure.

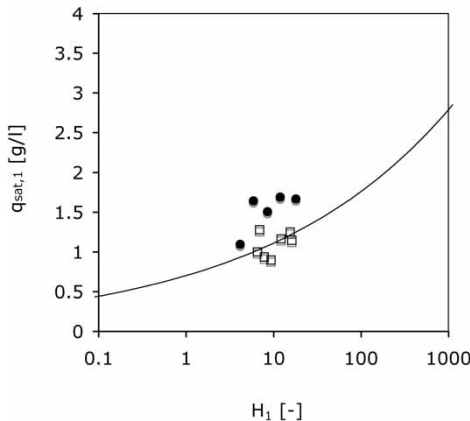


**Figure 14.** Saturation capacity for the first adsorption site of Calcitonin and Insulin as a function of the corresponding Henry constant of the first adsorption site evaluated on “Column 2” for  $x_{\text{H}_3\text{PO}_4} = 2.0 \text{ g/kg}$ . Filled circles: Insulin; squares: Calcitonin; curve: Eq. (13).

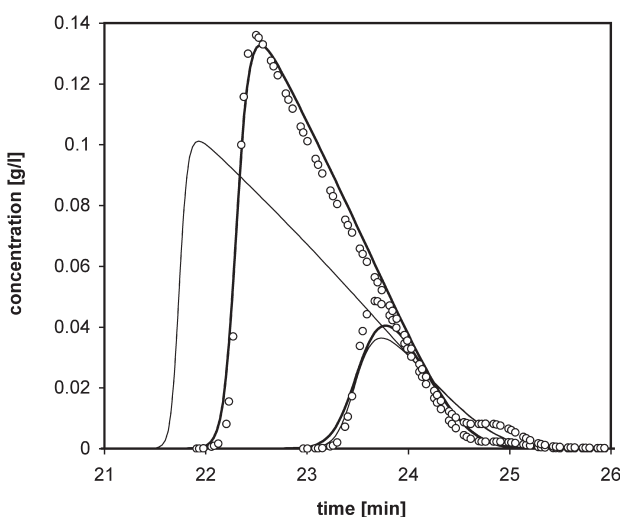


**Figure 15.** Comparison between predicted and experimental solvent gradient elution profiles of Insulin and simulated elution profiles of Calcitonin on “Column 2”. Thick line: simulations for Insulin (5 and 25  $\mu\text{l}$  of 7 g/l solution of Insulin). Thin solid curve: simulations for Calcitonin (5 and 25  $\mu\text{l}$  of 7 g/l solution of Calcitonin); circles: calibrated UV-signal for Insulin at 280 nm. Same modifier gradient as in Figure 8(d).  $Q = 1.0 \text{ ml/min}$ .

### Separation of Calcitonin-Insulin Mixture

Due to the good result obtained above for Insulin, it was decided to carry out a fictitious separation problem, where an overloaded linear gradient elution of a mixture of 16.5 g/l Calcitonin and 24 g/l Insulin on "Column 2" has been carried out. The modifier gradient applied is the same as in Fig. 15. A comparison between experimental and simulation results is shown in Fig. 16. As it can be observed, the model prediction very well overlap to the measured single elution profiles. Moreover, the sharp displacement effect of Calcitonin by Insulin is well predicted by the simulation model.

From this investigation using Insulin, it can be concluded that, even if peptides with very different properties are investigated, they show a surprisingly similar adsorption behavior on reverse phase columns, when the equilibrium parameters are scaled as a function of the individual overall Henry constants. This implies that, once a peptide is well characterized, it is possible to estimate the adsorption isotherm of a different peptide only by evaluating its overall Henry constant.

### Change in the Organic modifier

In the previous sections, it has been shown that, once a single peptide (Calcitonin) is well characterized and all its isotherm parameters are

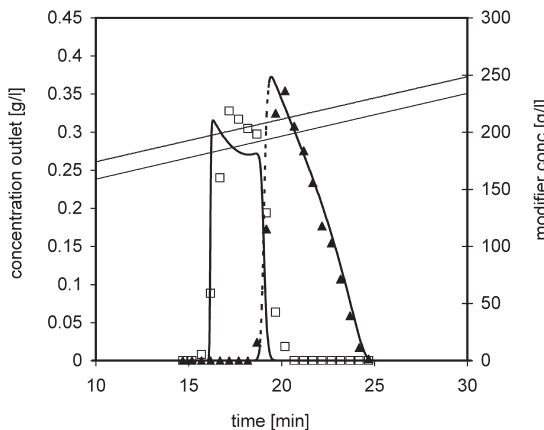


**Figure 16.** Comparison between simulated and experimental solvent gradient elution profiles for the injection of 50  $\mu$ l of a mixture of 40.5 g/l consisting of 59.3% Insulin and 40.7% Calcitonin on "Column 2". Same gradient as in Figure 15.  $Q = 1.0$  ml/min. Thin solid line: inlet modifier gradient; solid line: simulated modifier concentration at the column outlet; thick solid curve: simulated calcitonin concentration at the column outlet; dotted curve: simulated Insulin concentration at the column outlet; squares: experimental elution profile of Calcitonin; filled triangles: experimental elution profile of Insulin.

correlated to the overall Henry coefficient, it is possible to use the same correlations for different peptides (impurities). In all these cases, only the Henry coefficient of the different components as a function of the mobile phase composition must be estimated. In this section, the same approach has been used to estimate the effect of the change of the organic modifier in the mobile phase. In particular, ethanol will be used instead of acetonitrile. The acid content was kept constant ( $x_{\text{H}_3\text{PO}_4} = 2 \text{ g/kg}$ ). In these conditions, the total accessible porosity of Calcitonin does not significantly change.

In Fig. 17 the experimental overall Henry constant of Calcitonin evaluated using ethanol as a modifier (open squares) is compared with the one evaluated for acetonitrile. It can be seen, that the absolute value of the Henry constant does strongly differ for the two modifiers, but the qualitative behavior is very similar. The regressed parameters of Eq. (11) are reported in Table 2. It is worth mentioning that the diffusion coefficient regressed is about 3 times smaller than for acetonitrile as modifier. This is due to the higher viscosity of the ethanol water mixture. As a result, the pressure loss of the column increased by more than 200%.

An overloaded solvent gradient elution of the raw peptide mixture is carried out. In Fig. 18, the experimental chromatogram for Calcitonin and the key-impurities is compared with the simulated one, similarly to what has been done in Fig. 11 with acetonitrile as a modifier. The same selectivities of the impurities reported in Table 4 and evaluated for acetonitrile as modifier

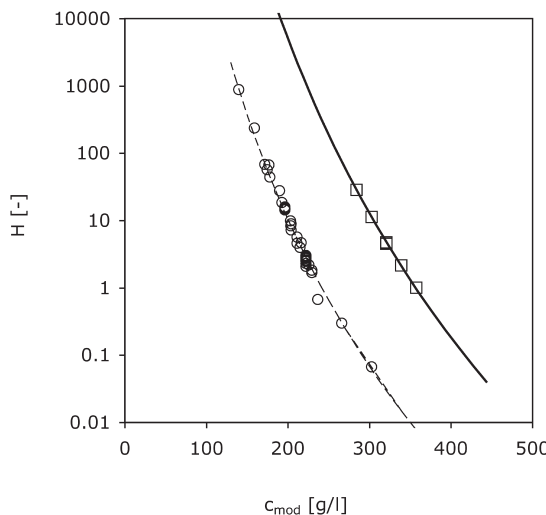


**Figure 17.** Comparison between the overall Henry constants of Calcitonin as a function of the concentration of acetonitrile and ethanol as modifiers. Squares: ethanol as modifier; circles: acetonitrile as modifier; thick solid curve: Eq. (11) for ethanol; dashed line: Eq. (11) for acetonitrile.

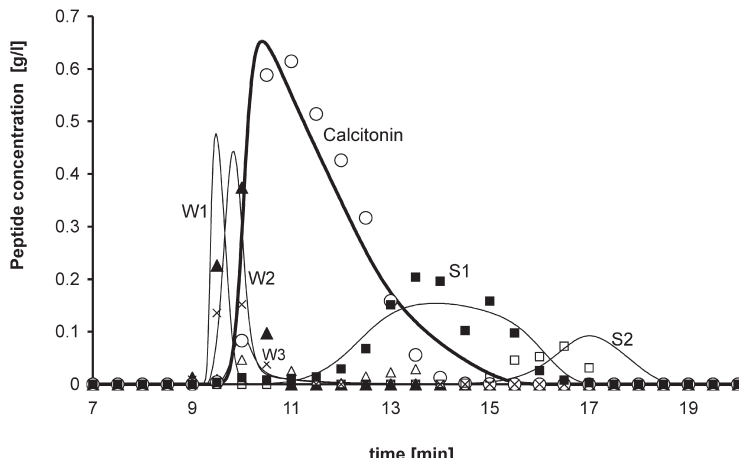


**Figure 18.** Simulated and experimental chromatograms for Calcitonin and weakly (W1, W2, and W3) and strongly (S1 and S2) impurities for a solvent gradient elution with ethanol as modifier. Gradient from 211 to 357.3 g/l in 15 minutes.  $Q = 1.0 \text{ ml/min}$ . Thin solid curves: simulation profiles of key impurities; thick solid curves: simulation profile of Calcitonin; crosses: impurity W1 (2% of feed); filled triangles: impurity W2 (7% of feed); empty triangles: impurity W3 (2% of feed); circles: Calcitonin (46% of feed); filled squares: impurity S1 (17% of feed); empty squares: impurity S2 (5% of feed).

are used in this model simulation. As it can be observed, the prediction of the gradient elution is again very accurate. The selectivities for the elution with ethanol seem to be very similar to the ones found for acetonitrile. Moreover, the peaks are less sharp and the displacement effects less pronounced, as it is clearly indicated by the offline analyses of fractions collected during the elution. This is the effect of the larger mass transport resistance found when using ethanol as organic modifier.

## CONCLUSION

In this work, a procedure is developed to characterize the adsorption behavior of a complex mixture of peptides, where Calcitonin is the main product, on polystyrene-based reverse phase columns. The procedure requires a limited experimental effort and a minimum amount of material, as it is needed in industrial applications, particularly in the clinical test phase of a new drug. The key-idea behind the suggested procedure is that different peptides may possess a relatively close adsorption behavior on this kind of stationary phases, in spite of the differences in their chemical structure and properties. In this case, it is possible to correlate the adsorption isotherm of different peptides to a single one and, more specifically, the isotherm of the different

impurities to that of the main component. As a result, by this procedure only a relatively small number of experiments is required, which is particularly important when the main product and especially the impurities are available only in small amounts.

According to the suggested procedure, the isotherm of the main component must be fully characterized first. Adsorption of Calcitonin is well described by a simple bi-Langmuir isotherm, in which all the involved parameters (Henry coefficient and saturation capacities of the two adsorption sites) vary with the mobile phase composition. The overall Henry coefficient can be regressed from isocratic diluted experiments. The other parameters, with the exception of the adsorption capacity of the second site, are instead regressed by isocratic adsorption experiments. It is found that the main component is more retained on the first adsorption site, but the saturation capacity of this site is small.

On the other hand, the saturation capacity of the second site is much larger, but its retention is significantly smaller. Therefore, the adsorption behavior of the second site in these experiments (where the total injected amount of Calcitonin is limited) is still in the linear range of the adsorption isotherm, while the one of the first site is already in the non-linear one. In order to reach non-linear adsorption conditions also on the second adsorption site, i.e. to approach its saturation conditions, gradient elution experiments are therefore needed, from which its saturation capacity can be then estimated. Finally, all the parameters are correlated to the overall Henry coefficient (and, through this to the mobile phase composition) using suitable power functions.

The same correlations are then applied to the impurities present in the original raw peptide mixture containing calcitonin, where the Henry coefficient of the main impurities are estimated by diluted isocratic experiments using the original raw mixture and, thus, without the need of isolating the impurities. To this regards, note that only the impurities eluting close to the main component need to be characterized, since these are the ones mostly interacting with the main component during overloaded experiments, due to displacement effects. Equally satisfactory results were obtained in this case, when the prediction of overloaded gradient experiments using the raw multi-component mixture in the presence of large displacement effects were compared to the experimental results. This successful comparison demonstrates the reliability of the suggested procedure and its potential as a tool for the design and optimization of preparative purifications of complex industrial peptide mixtures.

Equally good results have been obtained when a model peptide, Insulin, was used as main impurity. In particular, after having experimentally estimated the overall Henry constant of Insulin, the same correlations developed for calcitonin have been used to estimate all the remaining adsorption isotherm parameters for Insulin. Using these parameters values in the chromatographic model it was possible to correctly predict overloaded

gradient experiments, also in the presence of strong competition between the two peptides.

Finally, the same procedure has been successfully applied to the purification of Calcitonin, using ethanol in place of acetonitrile as a modifier. Also in this case, only the overall Henry constant of Calcitonin as a function of the ethanol content has been experimentally evaluated and overloaded gradient experiments using the raw mixture are accurately simulated.

The fact that both similar adsorption behaviors are obtained, both by changing the peptide and the modifier, suggests that adsorption is mostly influenced by how the modifier/solutes partition inside the pores of the stationary phase. Further investigations are however needed to clarify the reasons behind the success of the developed procedure.

## NOMENCLATURE

Name	Description	Unit
V	empty column volume	[ml]
v	volume	[ml]
$v_{\text{dead}}$	dead volume	[ml]
$v_{\text{dead,capil}}$	dead volume of capillaries	[ml]
$v_{\text{dead,mix}}$	internal dead volume of the pump	[ml]
L	column length	[mm]
$d_p$	average particle diameter	[cm]
D.I.	column inner diameter	[mm]
Q	volumetric flow rate	[ml/min]
$u_{\text{sf}}$	superficial velocity	[cm/s]
$\varepsilon$	total porosity	[—]
$\varepsilon_b$	external porosity	[—]
$\varepsilon_p$	internal porosity	[—]
H	overall Henry constant $H = H_1 + H_2$	[—]
$H_1$	Henry constant for site 1	[—]
$H_2$	Henry constant for site 2	[—]
$c_i$	liquid bulk concentration of component i	[g/l]
$c_p$	liquid pore concentration	[g/l]
$c_{\text{in}}$	liquid concentration, inlet	[g/l]
$q_{\text{sat}}$	saturation capacity	[g/l]
$q_{\text{sat},1}$	saturation capacity for site 1	[g/l]
$q_{\text{sat},2}$	saturation capacity for site 2	[g/l]
$q^*$	adsorbed overall equilibrium concentration	[g/l]
$q^*_1$	adsorbed equilibrium concentration for site 1	[g/l]
$q^*_2$	adsorbed equilibrium concentration for site 2	[g/l]
q	adsorbed concentration	[g/l]
$\bar{q}$	overall concentration in solid phase	[g/l]
$x_{\text{H}_3\text{PO}_4}$	liquid mass fraction of phosphoric acid	[g/g]

$t$	time [min]
$t_R$	retention time [min]
$t_0$	retention time under non adsorbing conditions [min]
$t_d$	dead time [min]
$k_L$	lumped liquid diffusion coefficient [1/s]
$k_f$	external film transfer coefficient [cm/s]
$\bar{k}_f$	specific external film transfer coefficient [1/s]
$\bar{k}_p$	effective pore diffusion coefficient [1/s]
$D_{\text{eff}}$	effective pore diffusivity [cm <sup>2</sup> /s]
$D_m$	molecular diffusivity [cm <sup>2</sup> /s]
$D_{\text{ax}}$	axial dispersion coefficient, $D_{\text{ax}} = D_{\text{ax}} u_{\text{sf}}$ [cm <sup>2</sup> /s]
$d_{\text{ax}}$	specific axial dispersion coefficient [cm]
$HETP$	Height of a Theroretical Plate [cm]
$W_{05}$	width at half height [min]
$\mu$	first order moment [-]
$\sigma$	second centered order moment [-]
$\gamma_1$	coefficient [-]
$\gamma_2$	coefficient [-]
$MW$	molecular weight [g/mol]
$Sh$	Sherwood number [-]
$Sc$	Schmidt number [-]
$Re$	Reynolds number [-]
$\eta$	viscosity [cP]
$\rho$	Density [g/l]
$A_{x,y}$	coefficient [-]
$B_{x,y}$	coefficient [-]
$D_{x,y}$	coefficient [-]
$A_{\text{qsat},1}$	coefficient [g/l]
$A_{\text{qsat},2}$	coefficient [g/l]

## ACKNOWLEDGMENTS

This work was financially supported by NOVARTIS Pharma AG, Basel, Switzerland.

## REFERENCES

1. Storti, G., Baciocchi, R., Mazzotti, M., and Morbidelli, M. (1995) Design of optimal operating conditions of simulated moving bed adsorptive operating units. *Ind. Eng. Chem. Res.*, 34: 288–301.
2. Aumann, L. and Morbidelli, M. (2005) European Patent Pending No: EP 05405327.7.

3. Guiochon, G., Golshan-Shirazi, S., and Katti, A.M. (1994) Fundamentals of preparative and nonlinear chromatography; Academic Press: Boston, MA.
4. Tondeur, D., Kabir, H., Luo, L., and Granger, J. (1996) Multicomponent adsorption equilibria from impulse response chromatography. *Chem. Eng. Sc.*, 51 (15): 3781–3799.
5. Dose, E.V., Jacobson, S., and Guiochon, G. (1991) Determination of isotherms from chromatographic peak shapes. *Anal. Chem.*, 63: 833–839.
6. Tju-Lik, N.G. and Soon, N.G. (1985) Computer simulation of abnormal high-performance liquid chromatograms caused by solvents. *J. Chromatogr. A*, 329: 13–24.
7. Golshan-Shirazi, S. and Guiochon, G. (1989) Experimental study of the elution profiles of high concentration bands of binary mixtures eluted by a binary eluent containing a strongly retained additive. *Anal. Chem.*, 61: 2380–2388.
8. Fallah, M.Z.E. and Guiochon, G. (1991) Gradient elution chromatography at very high column loading, effect of the deviation from the Langmuir model on the band profile of a single component. *Anal. Chem.*, 63: 2244–2252.
9. Fallah, M.Z.E. and Guiochon, G. (1992) Prediction of a protein band profile in preparative reversed-phase gradient elution chromatography. *Biotechnology and Bioengineering*, 39: 877–885.
10. Gu, T. and Zheng, Y. (1999) A Study of scale-up of reversed-phase liquid chromatography. *Separation and Purification Technology*, 15: 41–58.
11. Gu, T., Truei, Y.H., Tsai, G.J., and Tsao, G.T. (1992) Modeling of gradient elution in multicomponent nonlinear chromatography. *Chemical Engineering Science*, 47 (1): 253–262.
12. Ladiwala, A., Rege, K., Breneman, C.M., and Cramer, S.M. (2005) A priori prediction of adsorption isotherm parameters and chromatographic behavior in ion-exchange systems, *Proceedings of the National Academy of Sciences of the United States of America*, 102(33): 11710–11715.
13. Mant, C.T. and Hodges, S. (2002) Reversed-phase liquid chromatography as a tool in the determination of the hydrophilicity/hydrophobicity of aminoacid side-chains at a ligand receptor interface in the presence of different aqueous environments. Effect of varying receptor hydrophobicity. *J. Chromatogr. A*, 972 (1): 45–60.
14. Mant, C.T. and Hodges, S. (2002) Reversed-phase liquid chromatography as a tool in the determination of the hydrophilicity/hydrophobicity of amino acid side-chains at a ligand-receptor interface in the presence of different aqueous environments -II. Effect of varying peptide ligand hydrophobicity. *J. Chromatogr. A*, 972 (1): 61–75.
15. Chakraborty, C., Nandi, S., and Sinha, S. (2004) Overexpression, purification and characterization of recombinant salmon calcitonin, a therapeutic protein, in streptomyces avermitilis. *Protein and Peptide Letters*, 11 (2): 165–173.
16. Torres-Lugo, M. and Pes, N.A. (1999) Molecular design and in vitro studies of novel pH-sensitive hydrogels for the oral delivery of calcitonin. *Macromolecules*, 32: 6646–6651.